

**TASK: TW4-TTMI-003**  
**IFMIF, Test Facilities**

***Deliverable: Evaluation and validation of D-Li cross-section data: Up-dated evaluations of  $d+ {}^6,7\text{Li}$  data up to 50 MeV\****

*M. Avrigeanu<sup>1</sup>, W. von Oertzen<sup>2</sup>, U. Fischer<sup>3</sup>, and V. Avrigeanu<sup>1</sup>*

<sup>1</sup>*“Horia Hulubei” National Institute for Physics and Nuclear Engineering, Bucharest*

<sup>2</sup>*Freie Universität Berlin, Fachbereich Physics, Arnimallee 14, 14195 Berlin, and  
Hahn-Meitner-Institut, Glienicker Strasse 100, 14109 Berlin, Germany*

<sup>3</sup>*Institut für Reaktorsicherheit, Forschungszentrum Karlsruhe GmbH, Karlsruhe, Germany*

An analysis of the elastic scattering of deuterons on  ${}^6,7\text{Li}$ , for energies up to 50 MeV, has been carried out by using a phenomenological optical potential. Energy-dependent average parameters of the optical model potential have been involved also in the analysis of the corresponding real and imaginary volume integrals, pointing out an “anomalous” behavior of the real phenomenological potential when the imaginary part approaches zero. On the other hand, the coupled reaction channels method has been used in order to describe the  ${}^6\text{Li}(d,d_0){}^6\text{Li}$  experimental angular distributions within the backward hemisphere at 14.7 and 19.6 MeV but not at 50 MeV. The comparison of the experimental and calculated elastic-scattering angular distributions has proved the reliability of the present average optical potentials, with respect to the extrapolation of the use of deuteron global potentials outside of their mass and energy domains of definition.

## **1. Introduction**

The elastic scattering of deuterons on light nuclei has been less investigated mainly due to the difficulties to interpret it in terms of the usual optical-model potential (OMP). The cross sections often show considerable energy dependence or resonance structure, which implies that the coupling to some of the excited states of the target has to be considered explicitly. Also the level densities in the compound nuclei are low, and the optical model description may be rather poor because of insufficient averaging over the resonance states [1]. These aspects raise some questions about the reliability of the OMP for description of the elastic scattering of deuterons on light nuclei and were the reason that the exhaustive analysis devoted to the deuteron OMP by Daehnick et al. [2] concerned target nuclei heavier than  ${}^{27}\text{Al}$ . Also, the earlier global parameter set of Perey and Perey [3] did not extend its applicability for target nuclei within the atomic number  $Z$  below 12 while the Lohr-Haeberly [4] global OMP parameterization works for target nuclei with an atomic mass number  $A > 40$ .

Nowadays, recent technologies like the fusion reactor projects request high accuracy interaction cross sections of the deuterons with light nuclei among which  ${}^6,7\text{Li}$  are most

important. In order to improve the calculation of the D-Li neutron source term of the International Fusion Material Irradiation Facility (IFMIF) we have updated the  $d+{}^{6,7}\text{Li}$  data evaluation [5] by analysis of the elastic scattering of deuterons on  ${}^{6,7}\text{Li}$ , for energies up to 50 MeV, by using a phenomenological OMP. The previous analyses [6-12] of deuteron elastic scattering on  ${}^{6,7}\text{Li}$  proved the reliability of the corresponding optical potential. However, the systematic behavior of the OMP parameter energy dependence was not considered. It is why the present work looks in this respect for the average OMP parameters able to describe the bulk of deuteron elastic-scattering data on  ${}^{6,7}\text{Li}$  target nuclei, for the deuteron energies from 3 MeV up to 50 MeV (Sec. 2). The low energy experimental data of Lomabaard and Friedland [13] for the elastic scattering of deuterons on  ${}^7\text{Li}$  have not been considered in the present analysis due to the broad resonance at incident deuteron energies from 1 to 2 MeV (e.g., Figure 16 of Ref. [14]). The OMP analysis has been completed by the coupled reaction channels (CRC) method in Sec. 3, in order to describe the  ${}^6\text{Li}(d,d_0){}^6\text{Li}$  experimental angular distributions at 14.7 and 19.6 MeV within the backward hemisphere. Final discussion of results and the conclusions are given in Sec. 4.

## **2. Phenomenological optical potential analysis**

The optical potential involved in this work for deuterons on a target nucleus with the atomic mass number  $A$  has the standard form consisting of a Coulomb term, a real volume Woods-Saxon potential, an imaginary surface derivative Woods-Saxon potential, and a spin-orbit potential of the Thomas form. We have used the computer code SCAT2 [15] for the analysis of the angular distributions of elastic scattered deuterons on  ${}^{6,7}\text{Li}$  target nuclei (Figures 1 and 2). Unfortunately a  $\chi^2$  analysis, which would have been the optimal procedure, has not been possible due to the lack of numerical cross sections including the errors for all experimental data involved in the present work. However, the good overall agreement finally obtained with the bulk of the experimental data for both target nuclei can be considered as a suitable validation of the actual potential parameter set. The only main questionable point concerns the  ${}^6\text{Li}(d,d_0){}^6\text{Li}$  experimental angular distributions at 14.7 and 19.6 MeV that are not properly accounted for within the backward hemisphere (Figure 1), in spite of even large changes of the corresponding OMP parameters with respect to their average trend.

The common feature of the experimental elastic scattering angular distributions of deuterons on  ${}^{6,7}\text{Li}$  (Figures 1 and 2) is a strong backward enhancement. The same behavior was reported by Igo et al. [16] within the study of the 11.8 MeV deuterons scattered on C, Al and Mg targets. In order to describe this peculiar behavior of angular distributions, Abramovich et al. [6] used spin-orbit depth  $V_{\text{SO}}$  values increased up to four times the typical phenomenological values ( $\sim 8$  MeV). We found a similar deep spin-orbit potential in a previous analysis [17] based on a semi-microscopic optical potential. However, since the missing of corresponding polarization data, we cannot find any justification for such a strong spin-orbit interaction that could only hide some other specific feature of the deuteron interaction with  ${}^{6,7}\text{Li}$ . On the other hand, apart from the large non-locality and low binding energy (2.22 MeV) of the deuteron, the difficulty of the elastic-scattering OMP analysis is increased by the concurrent breakup process too. The latter is favored by the cluster structure of both Lithium isotopes and the corresponding small separation energies of 1.48 MeV and 2.45 MeV for the systems  ${}^6\text{Li}=d+\alpha$  and, respectively,  ${}^7\text{Li}=t+\alpha$ . In this respect the experimental backward

rise in the angular distribution of the elastic channel could be the signature of the well-known elastic-transfer process [18] from the target nucleus to the projectile, which should be considered at least for the target nucleus  ${}^6\text{Li}$ . Therefore we did not strengthen in the present work the role of the spin-orbit potential but have kept both its depth and geometry parameters in the range of the phenomenological average values. Thus, the common constant values  $V_{\text{so}}=8$  MeV and  $r_{\text{so}}=0.86$  fm have been adopted for both target nuclei while a spin-orbit diffuseness  $a_{\text{so}}$  increasing with energy has been considered for  ${}^6\text{Li}$  target at the same time with a constant value  $a_{\text{so}}=0.25$  fm which has resulted from the  $d+{}^7\text{Li}$  elastic-scattering analysis.

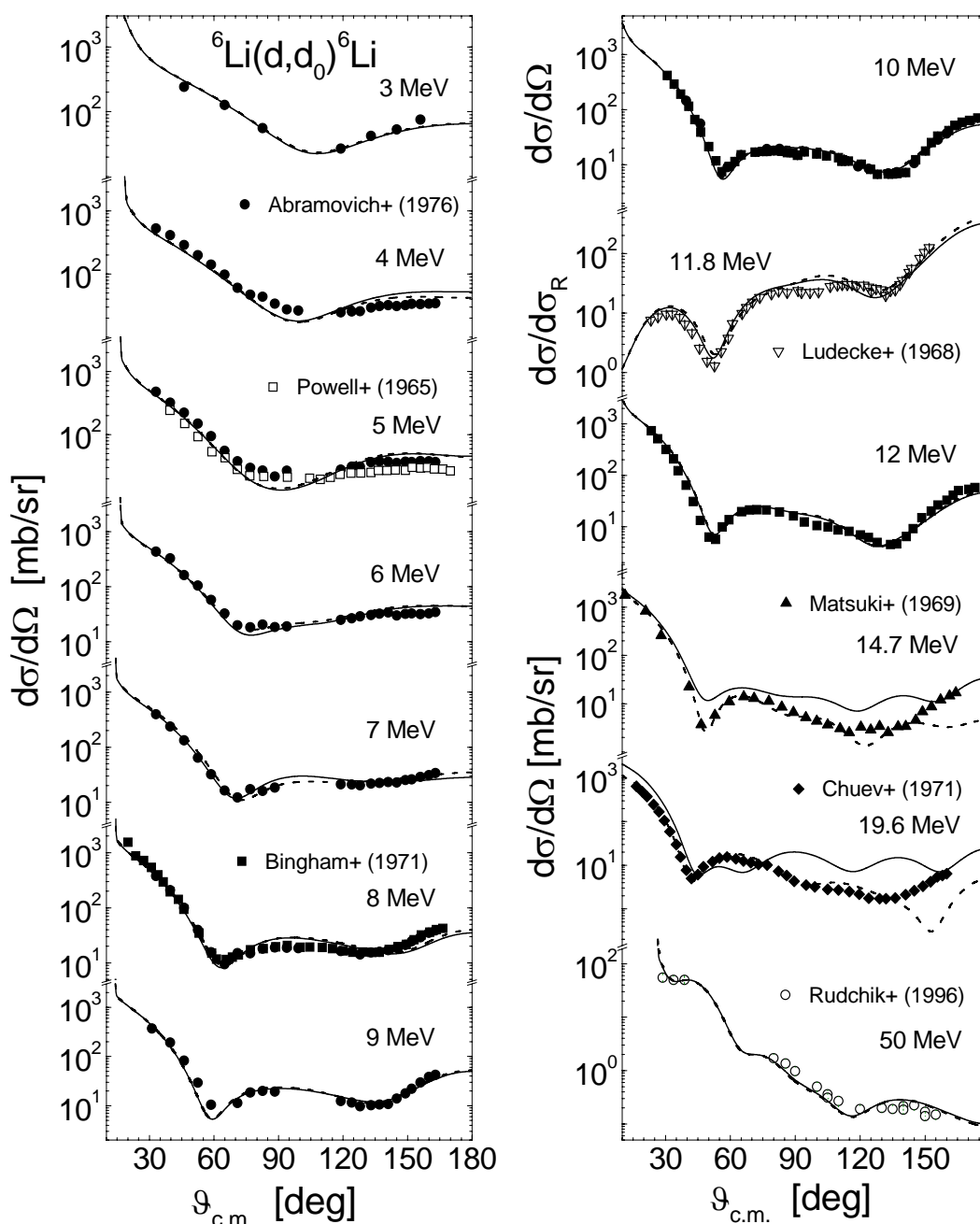


Figure 1. Comparison of the experimental [6-10,12] and calculated angular distributions of the elastic scattering of deuterons on  ${}^6\text{Li}$  between 3 and 50 MeV by using the present particular (dashed curves) as well as average (solid curves) phenomenological potential parameters.

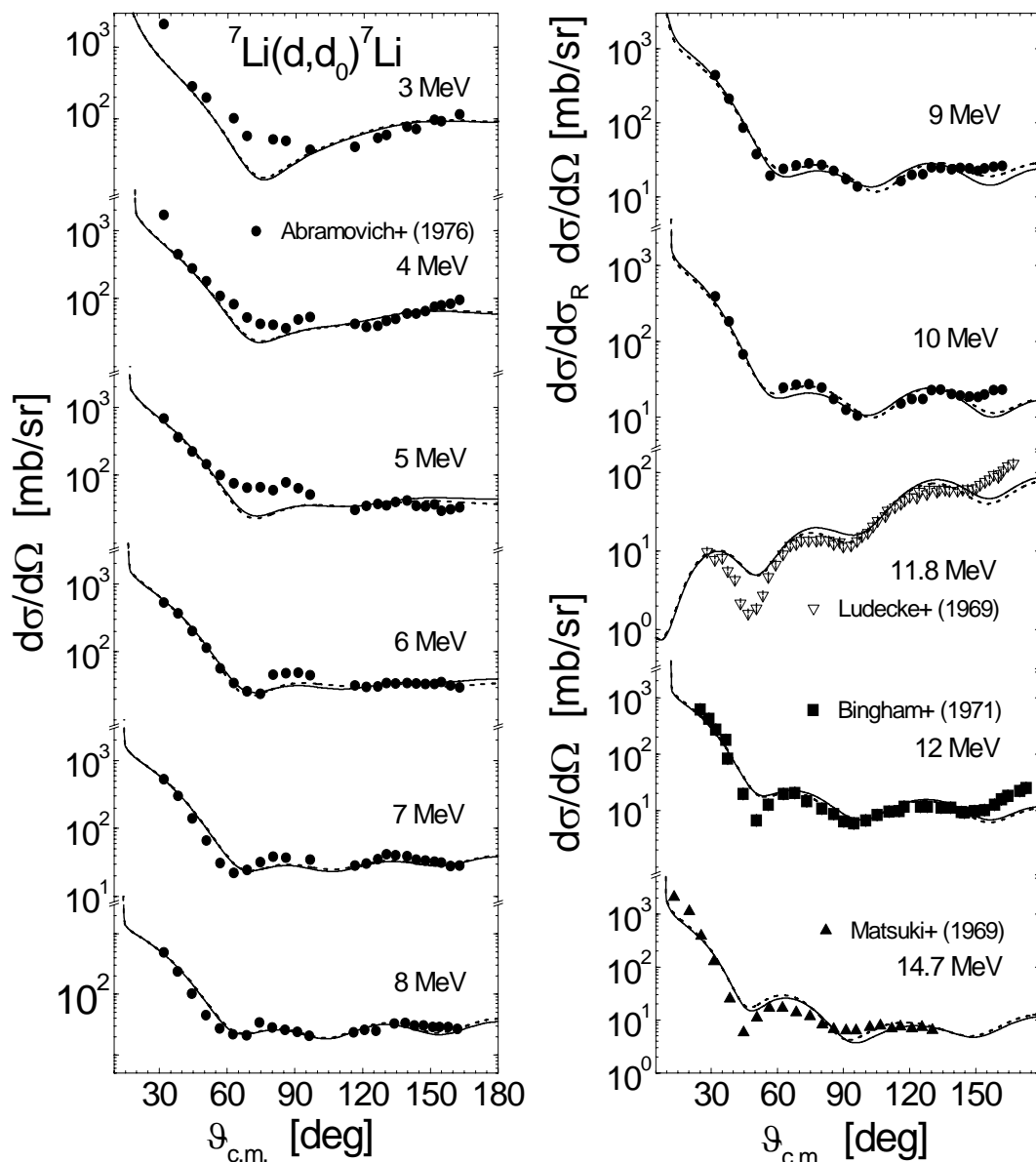


Figure 2. The same as in Figure 1 but for the target nucleus  ${}^7\text{Li}$  [6-9] and energies from 3 and 14.7 MeV.

The real and imaginary potential parameter values as well as the spin-orbit potential diffuseness have been obtained by the fit of experimental data. Their fit excepting the values corresponding to  ${}^6\text{Li}(d,d_0){}^6\text{Li}$  at the energies of 14.7 and 19.6 MeV, where the OMP description is found poor, has provided the average energy dependence of these OMP parameters (Figures 1 and 3 of Ref. [17]). Since for  $d+{}^7\text{Li}$  system there are available experimental elastic-scattering angular distributions up to only 14.7 MeV, an OMP average parameter extrapolation to 50 MeV has been carried out in this case in close connection with the corresponding features following the  $d+{}^6\text{Li}$  analysis. Thus, the energy dependence of the real potential depth has been considered up to 50 MeV, while the depth of the imaginary potential as well as the geometry parameters were taken constant above 14.7 MeV.

The elastic-scattering angular distributions calculated by using the average parameter set are also compared (Figures 1 and 2) with the experimental data and the former fit results corresponding to the particular parameters. A similar good overall agreement has been again obtained, providing a suitable validation of the average potential too, excepting again

the experimental angular distributions at 14.7 and 19.6 MeV on  ${}^6\text{Li}$  target nucleus. The increased disagreement resulting when the average parameters have been involved at these energies has pointed out the need for consideration of an additional mechanism, i.e. the elastic-transfer processes discussed in the following section.

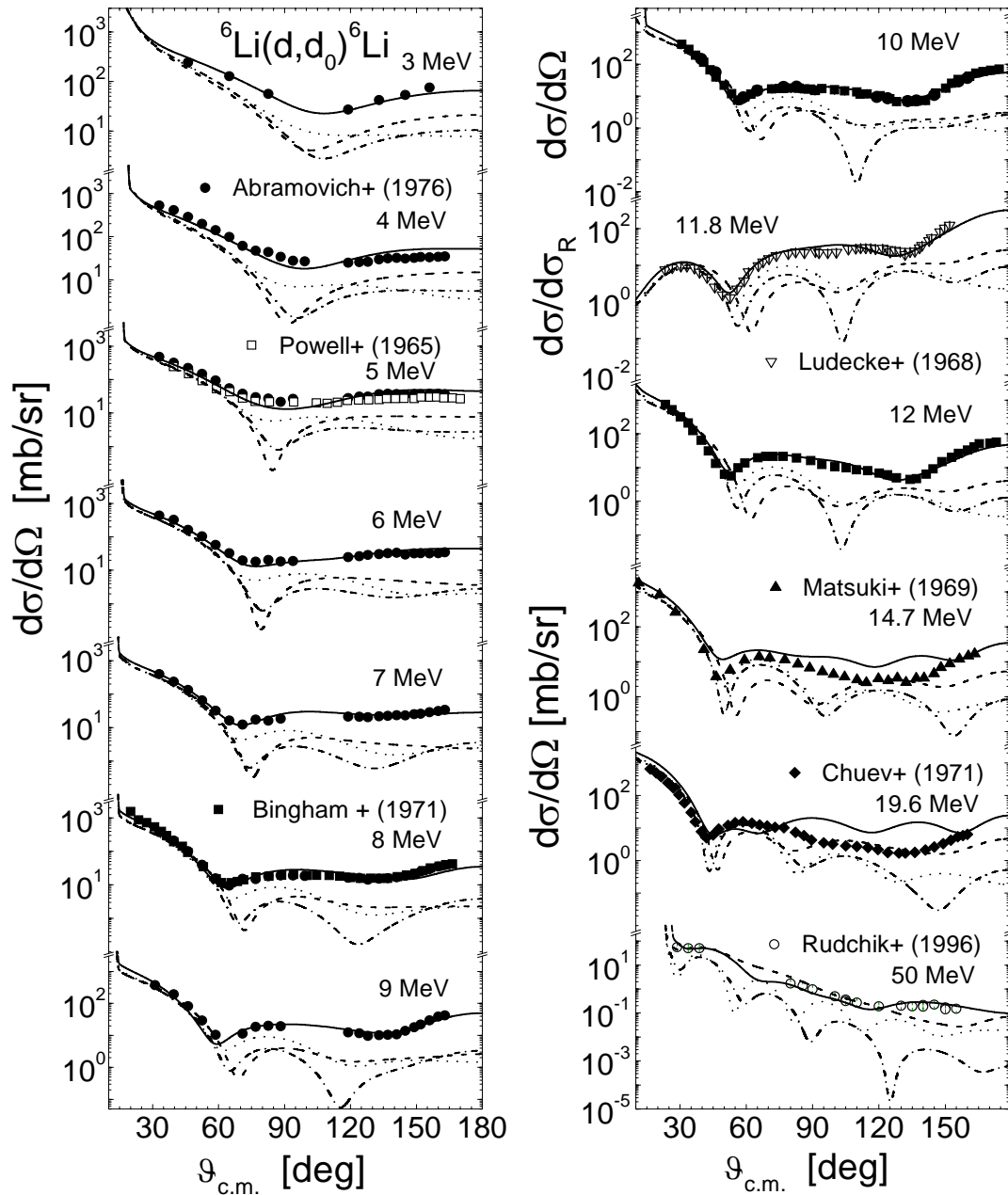


Figure 3. Comparison of the experimental [6-10,12] and calculated angular distributions of the elastic scattering of deuterons on  ${}^6\text{Li}$  between 3 and 50 MeV by using the present average optical potential parameters (solid curves) as well as the global parameter sets of Daehnick et al. [2] (dashed curves), Perey-Perey [3] (dot-dashed curves) and Lohr-Haerberli [4] (dotted curves).

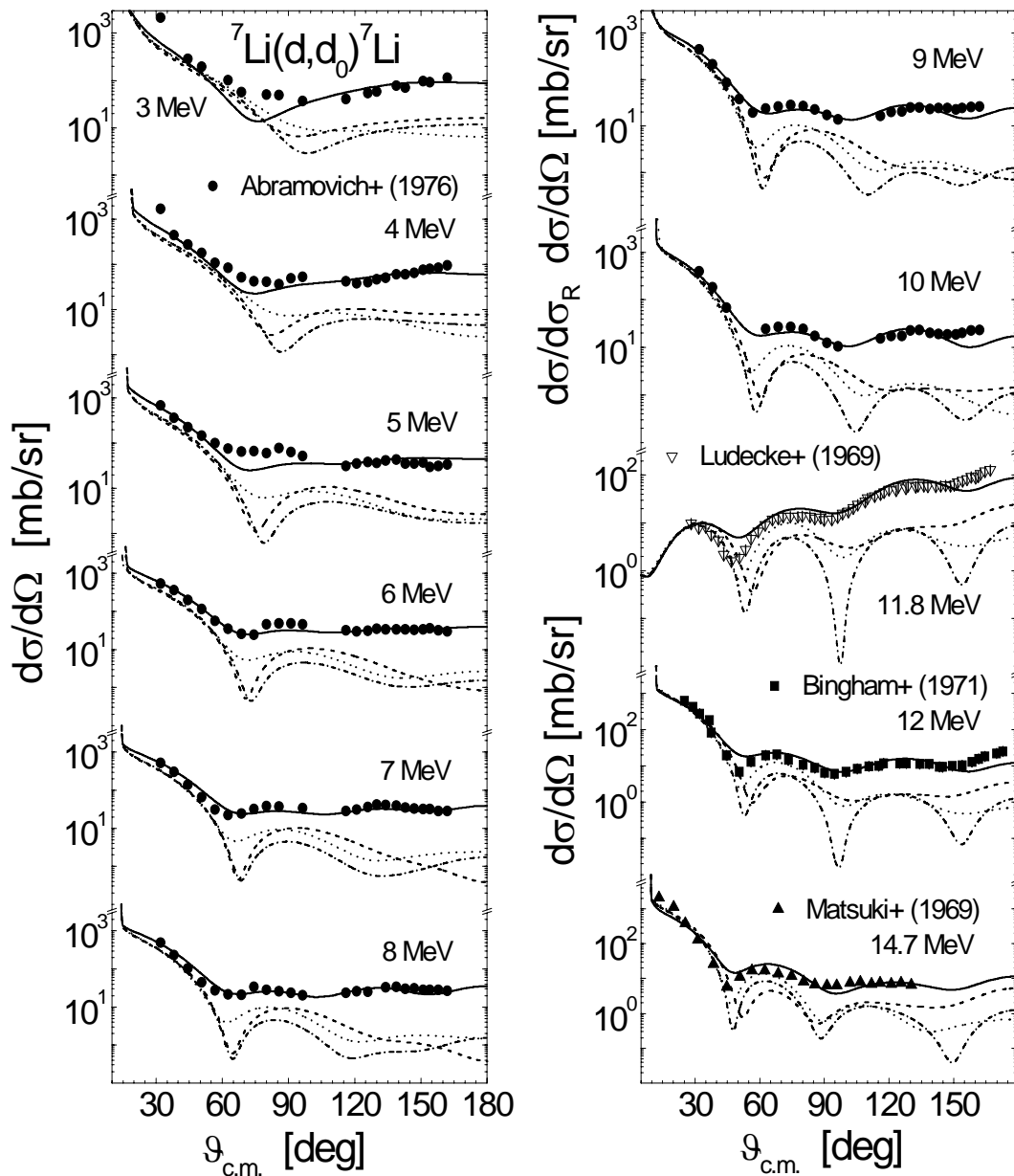


Figure 4. The same as in Figure 3 but for the target nucleus  ${}^7\text{Li}$  [6-9] and energies between 3 and 14.7 MeV.

Moreover, one may find that deviations of even our average parameter-set predictions from the experimental elastic-scattering angular distributions are almost negligible with respect to those of the widely-used deuteron global OMP parameter sets. Thus it is shown in Figures 3 and 4 that neither Lohr-Haeberli [4] and Daehnick et al. [2] nor Perey-Perey [3] parameter sets may describe the backward behavior of the experimental angular distributions either with or without a spin-orbit potential. Therefore, it results that an extrapolation of these global parameter sets to energies and target masses outside their data bases is not successful, while the average OMP obtained in the present work provides a suitable description of the experimental data for the target nuclei  ${}^{6,7}\text{Li}$ .

The energy dependence of the real  $J_R(E)$  and imaginary surface  $J_D(E)$  volume integrals per interacting nucleon pair has been analyzed too, for the general discussion and for comparison with other works. A striking energy dependence is shown by the volume integral of the present real OMP in comparison with the global parameter sets. Thus one may



consider that the real potential volume integral for the  $d+{}^6\text{Li}$  system shows the “anomaly” at low energies predicted by Mahaux et al. [19] for the nucleus-nucleus potential, i.e. a bell-shaped maximum for the real potential when the imaginary part approaches zero. The difference in this case is given by the energy range that is well above the top of the Coulomb barrier, where the sharp increase of the imaginary potential has been interpreted as due to the opening of the reaction channels with increasing available energy. However, the imaginary-potential volume integral still increasing up to 15 MeV for the  $d + {}^6\text{Li}$  system could be related to the particular structure of the  ${}^8\text{Be}$  nucleus, and finally to the maximum of the corresponding real potential as a consequence that they obey the dispersion relations [19]. This consideration could be supported also by the weak contribution from the breakup channel, which has been evidenced in present work by the pure elastic scattering description of the backward angular distributions. On the other hand, the decrease of the real potential of deuterons on  ${}^6\text{Li}$  at low energies could be also related to the non-locality of the basic real potential term which otherwise is at most slowly and smoothly energy-dependent. Nevertheless, this low energy “anomalous” behavior of the real phenomenological potential will be carefully taken into account in the completion of a semi-microscopic [17] analysis of the elastic scattering of deuterons on  ${}^{6,7}\text{Li}$ , in order to clarify both questions of the spin-orbit potential strength and possible non-locality correction to the double-folding real potential.

At the same time, a similar anomaly has been reported by the analyses made for a  ${}^7\text{Li}$  projectile interacting with heavy target nuclei [20,21] but is absent in the present case of the  $d + {}^7\text{Li}$  system. This absence could be however explained by the existence [16] of a large resonance in the low energy region (1-2 MeV).

### **3. CRC analysis of the $d+{}^6\text{Li}$ elastic scattering**

The failure of the OMP analysis to describe the  ${}^6\text{Li}(d,d_0){}^6\text{Li}$  experimental angular distributions at 14.7 and 19.6 MeV within the backward hemisphere (Figure 1) at once with smaller cross-section values, by using both particular and average parameter sets, pointed out the need for consideration of the additional mechanism of the well-known elastic-transfer process [22]. It is in this case the elastic  $\alpha$ -transfer following the  ${}^6\text{Li}$  breakup, indistinguishable experimentally from the elastic channel, which is affecting the scattering mainly at backward angles. We have taken into account this mechanism in the frame of the coupled reaction channels [23] (CRC) method.

The CRC calculations have been carried out with the version FRXY.1h of the computer code FRESKO [23] where the parameters of Timofeyuk et al. [24] for the bound states wave functions of the  $\alpha$ -particle and deuteron in  ${}^6\text{Li}$  as well as Yoshimura et al. [25]. Spectroscopic amplitude  $S_{lsj}$  have been used for calculation of the overlap integrals  $\langle \Psi_d | \Psi_{6\text{Li}} \rangle$ . The coupling to the first excited state of  ${}^6\text{Li}$  (Figure 5) and the reorientation processes ( $3^+-3^+$ ) have been calculated with the collective form factor [23], the deformation parameter being obtained from the empirical transition rate  $B(E2)$  [14].

The OMP parameters have been refitted in order to reproduce the elastic-scattering cross sections at forward angles while the sum of the elastic scattering and elastic  $\alpha$ -transfer is describing the backward part of the angular distribution. The adoption of the CRC method

makes possible the explicit treatment of the  ${}^6\text{Li}$  target higher-order effects, the target cluster structure ( $d+\alpha$ ) as well as the coupling to the deformed first excited state shown in Figure 5(a). An improved description of the backward cross sections has thus been obtained at both energies 14.7 and 19.6 MeV, with respect to the pure elastic scattering OMP calculations (Figure 5). It is obvious that the difference between the pure elastic scattering and the CRC calculations is not significant at small angles but proves to be important in the backward hemisphere. In addition to the CRC results for the elastic scattering it is also shown in Figure 5(c) the comparison of the experimental data and the CRC calculations corresponding to the inelastic scattering of 14.7 MeV deuterons on the first excited state of  ${}^6\text{Li}$ . There is however a disagreement at forward angles, where the decrease of the experimental inelastic scattering angular distribution is not described by the present calculations. Unfortunately the lack of additional experimental data is still preventing the enlightenment of this behavior of the inelastic angular distribution at forward angles.

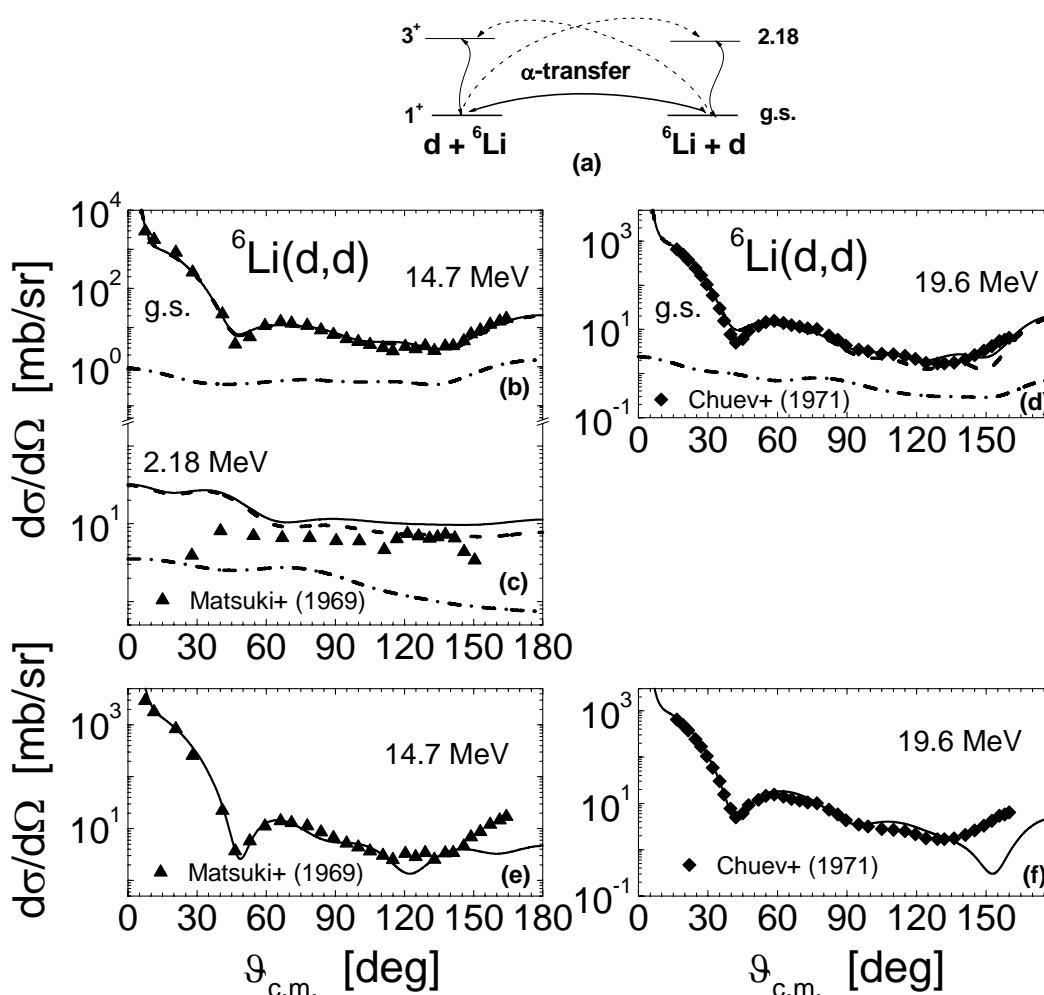


Figure 5. (a) Coupling diagram for deuteron-induced elastic  $\alpha$ -transfer (solid curve) and inelastic- $\alpha$  transfer to the  $3^+$  state of  ${}^6\text{Li}$  (dotted curves); comparison of CRC calculations and experimental (b) 14.7 MeV deuteron elastic- and (c) inelastic-scattering on  $3^+$  excited state of  ${}^6\text{Li}$  [9], and (d) 19.6 MeV deuteron elastic scattering on  ${}^7\text{Li}$  [11]; as well as comparison of optical model calculations for the pure elastic-scattering angular distributions of deuterons on  ${}^6\text{Li}$  at (e) 14.7 MeV and (f) 19.6 MeV and the corresponding experimental data [9,11].



On the other hand, we have found that the experimental elastic-scattering angular distribution for 50 MeV deuterons incident on  ${}^6\text{Li}$  does not exhibit any backward rise, as long as the experimental data [12] are measured only up to  $155^\circ$ , and the pure OM elastic scattering calculation has been enough for their description (Figure 1). The need for CRC calculations at the energies of 14.7 and 19.6 MeV but not at 50 MeV seems to be similar with the case of the  $\alpha$ -particles elastic scattering on  ${}^6\text{Li}$  analyzed by Goldberg et al. [26], following the decreasing of the probability for the exchange effects with increasing the incident energy of the incident particle.

#### **4. Discussion and conclusions**

The angular distributions of elastic scattered deuterons on  ${}^{6,7}\text{Li}$  target nuclei have been studied and the energy-dependent phenomenological OMPs up to 50 MeV have been obtained. Since the highest energy of the available experimental data for  $d+{}^7\text{Li}$  system is 14.7 MeV, an OMP parameter extrapolation up to 50 MeV has been proposed in close connection with the results of the  $d+{}^6\text{Li}$  analysis too. This enlarged extrapolation, following the lack of cross-section measurements, remains the single guidance for the nuclear data evaluation requested by the engineering design of the actual fusion test facilities.

On the other hand it is apparent that the difference between the OMP parameter sets corresponding to  ${}^{6,7}\text{Li}$  isotopes cannot be correlated with their charge asymmetry or mass-number change. This result may be explained by the effects of the structure particularities of the two target nuclei. Therefore, apart from the common feature of weakly bound nuclei of both the deuteron projectile as well as the cluster target nuclei  ${}^6\text{Li} = \alpha+d$  and  ${}^7\text{Li} = \alpha+t$ , some structural dissimilarities among the two Lithium isotopes seems to become important at the low incident energies of 3-15 MeV. Thus, the  ${}^6\text{Li}$  nucleus is spherical in its ground state and its dissociation energy 1.48 MeV is lower than the energy 2.185 MeV of its first (unbound) highly deformed excited state. However, the presence of the deuteron as a sub-cluster structure of the  ${}^6\text{Li}$  target has to be considered explicitly in the analysis of the deuteron interaction by adding the elastic  $\alpha$ -transfer contribution to the elastic-scattering angular distributions. The results of the CRC calculation for  $d + {}^6\text{Li}$  at 14.7 and 19.6 MeV have proved that it is thus provided a better description of the experimental data with respect to the consideration of only pure OM elastic scattering. In opposition to the  ${}^6\text{Li}$  ground state, the  ${}^7\text{Li}$  nucleus is highly deformed in its ground state while the dissociation energy of 2.45 MeV is also higher than that of the first excited state at 0.4776 MeV, strongly coupled to the ground state. These structure particularities may explain the experimental angular distributions that are so different, and underline the necessity of careful OMP analysis for very light systems. On the same basis should be understood the limited suitability of the deuterons global optical potentials [2,3] for the target nuclei below the range of  ${}^{24}\text{Mg}$ - ${}^{27}\text{Al}$ . Finally, the comparison with the experimental elastic-scattering angular distributions has proved the reliability of the calculations based on the use of the present average OMPs, with respect to the extrapolation of the use of the deuteron global potentials [2-4] outside of their mass and energy domains of definition.

## Acknowledgements

One of the authors (M.A.) acknowledges the hospitality of the Hahn-Meitner-Institut Berlin, and the Institut für Reaktorsicherheit, Forschungszentrum Karlsruhe, and useful discussion with Prof. Helmut Leeb.

## References:

- [1]. **Satchler G.R.**, Nucl. Phys. 85 (1966) 273.
- [2]. **Daehnick W.W., Childs J.D., Vrcelj Z.**, Phys. Rev. C 21 (1980) 2253.
- [3]. **Perey C.M., Perey F.G.**, Phys. Rev. 132 (1963) 755.
- [4]. **Lohr J.M., Haerberli W.**, Nucl. Phys. A232 (1974) 381.
- [5]. **Konobeyev A.Yu., Korovin Yu.A., Pereslavl'tsev P.E., Fischer U., and von Mollendorff U.**, Nucl. Sci. Eng. 139 (2001) 1.
- [6]. **Abramovich S.N., Guzjovskii B.Ya., Dzyuba B.M., Zvenigorods A.G., Trusillo S.V., Sleptsov G.N.**, Yad. Phys. 40 (1976) 842, and EXFOR-A0117 data file entry
- [7] **Bingham H. G., Zander A. R., Kemper K. W., Fletcher N. R.**,  
Nucl. Phys. A173 (1971) 265, and EXFOR-A1431 data-file.
- [8] **Ludecke H., Tan Wan-Tjin, Werner H., Zimmerer J.**, Nucl. Phys. A109 (1968) 676, and EXFOR-F0002 data-file entry.
- [9]. **Matsuki S., Yamashita S., Fukunaga K., Nguyen D.C., Fujiwara N., Yanabu T.**, Jap. Phys. J. 26 (1969) 1344, and EXFOR-A1435 data-file entry.
- [10]. **Powell D.L., Crawley G.M., Rao B.V.N., Robson B.A.**, Nucl. Phys. A147 (1970) 65, and EXFOR-A1432 data-file entry.
- [11]. **Chuev V. I., Davidov V. V., Novatsky B. G., Oglobin A. A., Sakuta S. B., and Stepanov D. N.**, J. de Phys. 32 (1971) C6.
- [12]. **Rudchik A.T., Budzanowski A., Koshchy E.I., Glowacka L., Mashkarov Yu.G., Makowska-Rzeszutko M., Pirnak Val. M., Siudak R., Szczurec A., Turkiewicz, Uleshchenko V.V.J., Ziman V.A.**, Nucl. Phys. A602 (1996) 211.
- [13]. **Lombaard J.M. and Friedland E.**, Z. Phys. 268 (1974) 413, and EXFOR-A1472 data-file entry.
- [14]. **Ajzenberg-Selove F.**, Nucl. Phys. A490 (1988) 3.

- [15]. **Bersillon O.**, Centre d'Etudes de Bruyeres-le-Chatel, Note CEA-N-2227, 1992.
- [16]. **Igo G., Lorentz W., Schmidt-Rohr U.**, Phys. Rev. 124 (1961) 832.
- [17]. **Avrigneanu M., von Oertzen W., Fischer U., and Avrigneanu V.**, Proc. Int. Conf. on Nuclear Data for Science and Technology, Sept. 26- Oct. 1, 2004, Santa Fe, USA (in press); Nucl. Phys. A (in press).
- [18]. **von Oertzen W., Bohlen H.G.**, Phys. Rep. 19C (1975) 1.
- [19]. **Mahaux C., Ngo H., Satchler G.R.**, Nucl. Phys. A449 (1986) 354.
- [20]. **Keeley N., Bennet S.J., Clarke N.M., Fulton B.R., Tungate G., Drumm P.V., Nagarajan M.A., Lilley J.S.**, Nucl. Phys. A571 (1994) 326.
- [21]. **Maciel A.M.M., Gomes P.R.S., Lubian J., Anjos R.M., Cabezas R., Santos G.M., Muri C., Moraes S.B., Liguori Neto R., Added N., Carlin Filho N., Tenreiro C.**, Phys. Rev. C 59 (1999) 2103.
- [22]. **von Oertzen W. and Bohlen H.G.**, Phys. Rep. 19 (1975) 2.
- [23]. **Thompson I.J.**, Comput. Phys. Rep. 7 (1988) 167.
- [24]. **Timofeyuk N.K., Thompson I.J.**, Phys. Rev. C 61 (2000) 044608.
- [25]. **Yoshimura T., Okihana A., Warner R.E., Chant N.S., Roos P.G., Samanta C., Kakigi S., Koori N., Fujiwara M., Matsuoka N., Tamura K., Kubo E., Ushiro K.**, Nucl. Phys. A641 (1998) 3.
- [26]. **Goldberg V. Z., Gridnev K. A., Hefter E. F., and Novatskii B. G.**, Phys. Lett. 58B (1975) 405.